Citation: CPT Pharmacometrics Syst. Pharmacol. (2019) 8, 396–406; doi:10.1002/psp4.12398

ARTICLE

Physiologically-Based Pharmacokinetic Modeling Analysis for Quantitative Prediction of Renal Transporter–Mediated Interactions Between Metformin and Cimetidine

Kotaro Nishiyama[1], Kota Toshimoto[2], Wooin Lee[3], Naoki Ishiguro[1], Bojan Bister[1] and Yuichi Sugiyama[2,*]

Metformin is an important antidiabetic drug and often used as a probe for drug–drug interactions (DDIs) mediated by renal transporters. Despite evidence supporting the inhibition of multidrug and toxin extrusion proteins as the likely DDI mechanism, the previously reported physiologically-based pharmacokinetic (PBPK) model required the substantial lowering of the inhibition constant values of cimetidine for multidrug and toxin extrusion proteins from those obtained *in vitro* to capture the clinical DDI data between metformin and cimetidine.[1] We constructed new PBPK models in which the transporter-mediated uptake of metformin is driven by a constant membrane potential. Our models successfully captured the clinical DDI data using *in vitro* inhibition constant values and supported the inhibition of multidrug and toxin extrusion proteins by cimetidine as the DDI mechanism upon sensitivity analysis and data fitting. Our refined PBPK models may facilitate prediction approaches for DDI involving metformin using *in vitro* inhibition constant values.

Study Highlights

WHAT IS THE CURRENT KNOWLEDGE ON THE TOPIC?
☑ Metformin is an important antidiabetic drug and a probe drug to predict drug–drug interactions (DDI) mediated by renal transporters. The previously reported physiologically-based pharmacokinetic (PBPK) models required a substantial lowering of *in vitro* inhibition constant values to reproduce the observed DDI data, necessitating the development of PBPK models suitable for the bottom-up prediction of the DDI potential.

WHAT QUESTION DID THIS STUDY ADDRESS?
☑ This study aimed to develop a new PBPK model of metformin and to quantitatively predict DDI between metformin and cimetidine (an inhibitor of organic cation transporter 1/2 and multidrug and toxin extrusion proteins) using *in vitro* inhibition constant values.

WHAT DOES THIS STUDY ADD TO OUR KNOWLEDGE?
☑ The constructed PBPK model incorporated the metformin transport process driven by the membrane potential kept constant and achieved the quantitative prediction of DDI incurred by cimetidine using *in vitro* inhibition constant values. The simulation results also supported the inhibition of multidrug and toxin extrusion proteins by cimetidine as the DDI mechanism.

HOW MIGHT THIS CHANGE DRUG DISCOVERY, DEVELOPMENT, AND/OR THERAPEUTICS?
☑ This metformin PBPK model represents an important advancement in quantitatively capturing the DDI mediated by renal transporters using middle-out approaches.

Metformin is a first-line therapy for type 2 diabetes, but its response varies substantially, with about 30% of patients failing to achieve glycemic control[2,3] and the rare incidence of severe events of lactic acidosis.[4] As such, it is important to understand the factors contributing to interindividual variation in metformin response and to quantitatively predict the potential for drug–drug interactions (DDIs) involving metformin.

The pharmacokinetics of metformin has been well characterized. The oral bioavailability of metformin is 50–60%.[5–8] Metformin undergoes negligible hepatic metabolism, but it is mainly excreted intact into the urine; its renal clearance exceeds the glomerular filtration rate, indicating tubular secretion. With negligible plasma protein binding, metformin slowly distributes to erythrocytes.[6,9] Metformin exists ionized at physiological pHs, relying on transporters for its translocation across cell membranes. Metformin is transported by the organic cation transporters (OCTs), particularly OCT1 in the liver[10] and OCT2 in the kidney.[11] Multidrug and toxin extrusion proteins (MATEs), namely MATE1 and MATE2-K are also shown to mediate the extrusion of metformin from proximal

[1]Pharmacokinetics and Non-Clinical Safety Department, Nippon Boehringer Ingelheim Co., Ltd., Kobe, Hyogo, Japan; [2]Sugiyama Laboratory, RIKEN Baton Zone Program, RIKEN Cluster for Science, Technology and Innovation Hub, Yokohama, Kanagawa, Japan; [3]College of Pharmacy and Research Institute of Pharmaceutical Sciences, Seoul National University, Seoul, Korea. *Correspondence to: Yuichi Sugiyama (ychi.sugiyama@riken.jp)
Received: October 31 2018; accepted: February 6 2019. doi:10.1002/psp4.12398

renal tubular cells to urine.[12] These transporters harbor genetic variations, some of which can impact the pharmacokinetics and pharmacodynamics of metformin.[13–15]

Cimetidine is an inhibitor of OCT2 and MATEs and incurs DDIs with metformin; the coadministration of cimetidine increased the systemic exposure of metformin in plasma by ~ 50%, whereas it decreased the renal clearance of metformin by ~ 30%.[16,17] The inhibition of OCT2 by cimetidine had been initially suspected as the DDI mechanism, but it was deemed unlikely as the reported values of the OCT2 inhibition constant (Ki) for cimetidine (ranging from 72.6–510 μM[10,11]) are much higher than the maximal unbound plasma concentrations of cimetidine (C_{max}; ranging from 7.67–9.48 μM after the oral administration of 400 mg cimetidine).[18,19] The reported Ki values of cimetidine for MATEs range from 1.21–13.5 μM.[20–22] The results from the mouse study (*in vitro* and *in vivo*) also supported the inhibition of MATEs as a likely mechanism for the DDI between cimetidine and metformin.[21]

Physiologically-based pharmacokinetic (PBPK) modeling analysis allows for quantitative prediction of drug concentration-time profiles and enhances our mechanistic understanding of DDI.[1,23,24] For metformin, a minimal PBPK model was previously reported but with no consideration of transporter-mediated processes.[9] Later, whole-body PBPK models were developed with the mechanistic components reflecting transporter-mediated processes (by OCT1, OCT2, and MATEs), namely, the conventional model and the "electrochemical model" driven by dynamically changing electrochemical modulation.[1] To reproduce clinical DDI data, these models required a substantial lowering of the Ki values of cimetidine for transporters from the *in vitro* reported values: for the conventional model, the lowering of the Ki values for OCT1 and OCT2 nearly by 500-fold, and for the electrochemical model, the lowering of the Ki values for OCT1, OCT2, and MATEs by 8~18-fold.[1] Thus, there is a clear need to develop a PBPK model that can quantitatively predict DDIs involving metformin using Ki values obtained *in vitro*.

We developed a new metformin PBPK model by incorporating hepatic and renal transporter–mediated processes driven by the membrane potential, which is kept constant. Our PBPK model achieved quantitative prediction of DDIs between metformin and cimetidine using *in vitro* data, supporting the inhibition of MATEs by cimetidine as the major DDI mechanism.

MATERIALS AND METHODS

Development of the metformin PBPK model

We modified the previously reported model[1,25] by adding erythrocyte compartments and implementing changes in the kidney and the liver (**Figure 1a**). The physicochemical and pharmacokinetic parameters of metformin are summarized in **Table S1**, and relevant physiological parameters are summarized in **Tables S2 and S3**. Adipose, muscle, and skin are incorporated considering their contribution to the distribution volume. Rapid equilibrium was assumed using the tissue-to-plasma concentration ratios predicted *in silico*[26] by physicochemical properties.

Erythrocyte compartments. Considering its slow distribution to erythrocytes and time-dependent changes in blood-to-plasma concentration ratios,[6] the systemic circulation and capillary vessels in all tissues were divided into plasma and erythrocyte compartments. The distribution processes between plasma and erythrocytes are defined in Eqs. 1 and 2.

$$\frac{X_{erythro}}{dt} = k_{in,RBC} * X_{plasma} - k_{out,RBC} * X_{erythro}, \quad (1)$$

$$\frac{X_{plasma}}{dt} = -k_{in,RBC} * X_{plasma} + k_{out,RBC} * X_{erythro} \quad (2)$$

where $X_{erythro}$ and X_{plasma} are the amount of metformin in the erythrocyte and plasma compartment, respectively, and $k_{in,RBC}$ and $k_{out,RBC}$ are the partitioning rate constants of metformin from plasma to erythrocytes and from erythrocytes to plasma, respectively, and obtained *in vitro* by measuring time-dependent blood cell distribution of metformin using human blood[9] (**Table S1**).

Liver model. A five-compartment liver model was used as similar to our previous report.[24] Biliary excretion was not included in the model as clinical data indicated that metformin is not excreted into bile. Considering that OCT1 is a bidirectional transporter driven by the membrane potential, the OCT1-mediated transport is defined using Eq. 3,[27] the Michaelis–Menten constant ($K_{m,OCT1}$), and the maximum rate ($V_{max,OCT1}$).

$$\begin{aligned}\textbf{OCT1 transport} &= \mathbf{PS_{OCT1,inf}} * \boldsymbol{C_{EH}} - \mathbf{PS_{OCT1,eff}} * \boldsymbol{C_{HC}} \\ &= \mathbf{V_{max,OCT1}} * \left(\frac{\boldsymbol{C_{EH}}}{\boldsymbol{K_{m,OCT1}} + \boldsymbol{C_{EH}}} - \frac{\boldsymbol{e^N}}{\boldsymbol{R_{OCT1,inf/eff}}} * \frac{\boldsymbol{C_{HC}}}{\boldsymbol{K_{m,OCT1}} + \boldsymbol{C_{HC}}} \right) \end{aligned} \quad (3)$$

$$N = \frac{z * \Phi * F}{R * T} \quad (4)$$

where $PS_{OCT1,inf}$ and $PS_{OCT1,eff}$ are the intrinsic OCT1-mediated clearance via influx into and efflux out of hepatocytes, respectively; C_{HC} and C_{EH} are the metformin concentrations inside and outside hepatocytes, respectively; $R_{OCT1,inf/eff}$ is the OCT1-mediated influx-to-efflux ratio; z, Φ, F, R, and T are the valence, the membrane potential, Faraday's constant, the gas constant, and the absolute temperature, respectively. The definitions for the other parameters are provided in the **Supplemental Text**.

Kidney model. The kidney model comprised the glomerulus, the proximal tubule (further divided into the S1, S2, and S3 regions), the distal tubule, and the collecting duct. The proximal tubule, the distal tubule, and the collecting duct were further divided into the three subcompartments representing the blood vessels, cells, and the urinary lumen, similar to the previous report.[1] The active transport of metformin was assumed to occur only in the proximal tubule by OCT2 and MATEs at the basolateral and luminal sides, respectively. Reabsorption of metformin from the urinary lumen was assumed to be mediated by passive diffusion. Considering that OCT2 is a bidirectional transporter driven by the membrane potential, the transport process by OCT2 is defined using Eq. 5, the Michaelis–Menten constant ($K_{m,OCT2}$) and the maximum rate ($V_{max,OCT2}$).

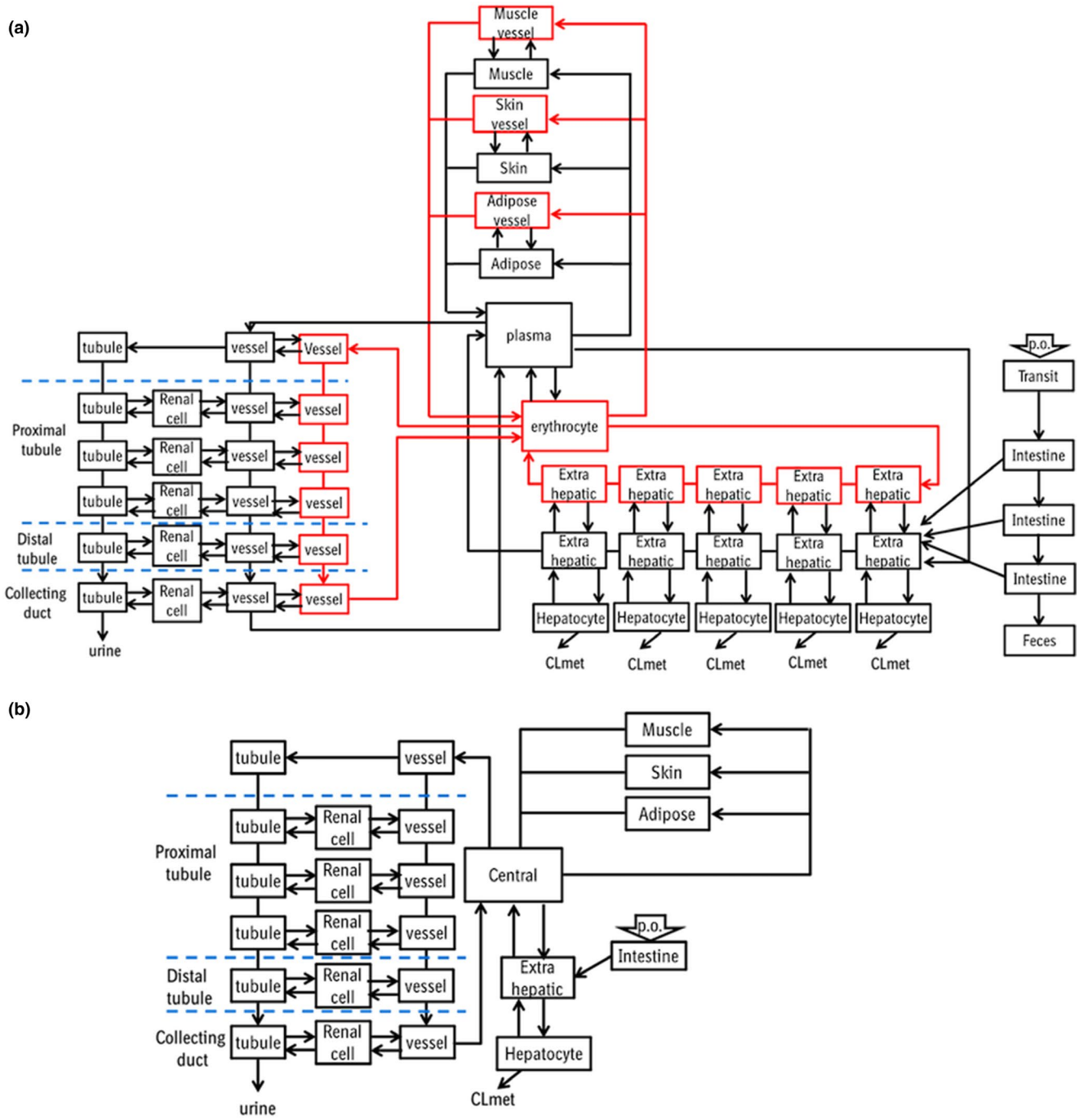

Figure 1 Structures of the physiologically-based pharmacokinetic models for metformin (**a**) and cimetidine (**b**). Erythrocyte compartments were incorporated into all the tissues in the metformin model (red boxes). CL_{met}, metabolic clearance; p.o., per os.

$$\begin{aligned}\textbf{OCT2 transport} &= \mathbf{PS_{OCT2,inf}} * \boldsymbol{C_r} - \mathbf{PS_{OCT2,eff}} * \boldsymbol{C_{rcell}} \\ &= \mathbf{V_{max,OCT2}} \\ &* \left(\frac{\boldsymbol{C_r}}{\boldsymbol{K_{m,OCT2}} + \boldsymbol{C_r}} - \frac{\boldsymbol{e^N}}{\boldsymbol{R_{OCT2,inf/eff}}} * \frac{\boldsymbol{C_{rcell}}}{\boldsymbol{K_{m,OCT2}} + \boldsymbol{C_{rcell}}} \right)\end{aligned} \quad (5)$$

where $PS_{OCT2,inf}$ and $PS_{OCT2,eff}$ are the OCT2-mediated intrinsic clearance via influx into and efflux out of renal cells, respectively; $R_{OCT2,inf/eff}$ is the influx-to-efflux ratio of OCT2; and C_r and C_{rcell} are the metformin concentrations in the blood vessels and renal cells, respectively.

As shown in Eq. 5, our model defined that the OCT2-mediated transport process is driven by a constant membrane potential, different from the previously reported PBPK model where the membrane potential changed in response to time-dependent changes in metformin concentrations.[1] The transporter-mediated processes in the liver were similarly

defined using the membrane potential kept constant. Intrinsic clearance by MATEs was defined using Eq. 6, the Michaelis–Menten constant ($K_{m,MATE}$) and the maximum rate ($V_{max,MATE}$).

$$PS_{MATE} = \frac{V_{max,MATE}}{K_{m,MATE}} + C_{in}. \quad (6)$$

In the proximal tubule, based on the extended clearance concept,[28] the parameters $CL_{int,sec}$, β_{kidney}, $R_{MATE/dif}$, γ_r, and γ_{urine} were defined using Eqs. 7–14:

$$CL_{int,sec} = PS_{r,inf} * \beta_{kidney} = PS_{r,inf} * \frac{PS_{urine}}{PS_{r,eff} + PS_{urine}} \quad (7)$$

$$\beta_{kidney} = \frac{PS_{urine}}{PS_{r,eff} + PS_{urine}} \quad (8)$$

$$R_{MATE/diff} = \frac{PS_{MATE}}{PS_{urine,dif,eff}} \quad (9)$$

$$\gamma_r = \frac{PS_{r,dif,inf}}{PS_{r,dif,eff}} = \frac{f_{o,union} + \lambda * f_{o,ion}}{f_{i,union} + e^N * \lambda * f_{i,ion}} \approx \frac{1}{e^N} = 13.7 \quad (10)$$

$$\gamma_{urine} = \frac{PS_{urine,dif,inf}}{PS_{urine,dif,eff}} \approx \frac{1}{e^N} = 12.3 \quad (11)$$

$$PS_{r,inf} = PS_{OCT2,inf} + PS_{r,dif,inf} \quad (12)$$

$$PS_{r,eff} = PS_{OCT2,eff} + PS_{r,dif,eff} \quad (13)$$

$$PS_{urine} = PS_{MATE} + PS_{urine,dif,eff} \quad (14)$$

where $CL_{int,sec}$ is the intrinsic urinary secretion clearance; $PS_{r,inf}$ and $PS_{r,eff}$ are the intrinsic renal clearance via influx into and efflux out of renal cells, respectively; PS_{urine} is the intrinsic efflux clearance from renal cells to the urinary lumen; $PS_{r,dif,inf}$ and $PS_{r,dif,eff}$ are the intrinsic passive clearance via influx into and efflux out of renal cells, respectively; $PS_{urine,dif,inf}$ and $PS_{urine,dif,eff}$ are the intrinsic passive clearance via influx into cells from the urinary lumen and efflux out of cells to the urinary lumen; $R_{MATE/dif}$ is the ratio of the intrinsic clearance of MATEs to the intrinsic passive diffusion clearance via efflux out of cells to the urinary lumen; γ_r and γ_{urine} are the passive influx-to-efflux ratio on the basolateral and luminal sides, respectively; λ is the ratio of passive diffusion for the ionized form to that for the unionized form; $f_{o,union}$ and $f_{o,ion}$ are the extracellular fractions of the unionized and ionized forms, respectively; $f_{i,union}$ and $f_{i,ion}$ are the intracellular fractions of the unionized and ionized forms, respectively; β_{kidney} is a hybrid parameter reflective of the major rate-limiting steps of $C_{Lint,sec}$

Metformin (pKa of 12.3) exists mainly ionized at physiological pHs (thus, $f_{o,union} = f_{i,union} = 0$ and $f_{o,ion} = f_{i,ion} = 1$), and γ_r and γ_{urine} were calculated using the Nernst equation.[29] Passive diffusion clearances of each compartment in the kidney were calculated using permeability measured in a parallel artificial membrane permeability assay system,[30] surface area, γ_r, and γ_{urine} (**Table S3**).[29,31]

Optimization of model parameters. Other unknown parameters (absorption rate constant, k_a; transit rate constant from the transit compartment to the intestinal compartment, k_{trans}; and $R_{MATE/dif}$) were optimized by fitting to the two clinical data sets obtained after oral administration of metformin at 1,500 mg (time profiles of plasma and blood concentrations and urinary excretion)[6] or 250 mg (DDI data between metformin and cimetidine).[16] Because reliable β_{kidney} was not estimated from the observed metformin pharmacokinetic data, four different β_{kidney} values (0.1, 0.3, 0.5, and 0.8) were used to cover a wide range of rate-determining step situations. Unknown parameters were optimized with β_{kidney} fixed (**Table 1**) and used as fixed values for DDI simulation. Under DDI conditions, the β_{kidney} value was not fixed and allowed to change as the renal transport processes became inhibited. Upon oral dosing, metformin showed a less than dose-proportional increase of area under the curve (AUC), suggesting saturable intestinal absorption processes.[32] To reflect such saturation, our PBPK model assumed that metformin is absorbed via first-order kinetics with the intestinal availability set as 0.57 and 0.84 for the metformin oral doses of 1,500 and 250 mg, respectively (back-calculated from the bioavailability data, **Table S1**). Between the two data sets (metformin oral doses of 250 mg and 1,500 mg),[6,16] time of maximum concentration (Tmax) values varied (3.3 and 1.5 hours, respectively). The reported T_{max} values vary substantially even with the same doses,[5,14,17] and the adjustment of T_{max} was deemed necessary in analyzing the two data sets together. As the same formulation was used in the two clinical studies,[6,16] the data of the 1,500 mg dose were used to obtain the optimized k_a value, which was then used for the data of the 250 mg dose. The k_{trans} and $R_{MATE/dif}$ values were optimized by fitting to the observed data after oral dosing of 250 mg metformin[16] using varying β_{kidney} values (0.1, 0.3, 0.5, and 0.8).

Development of the cimetidine PBPK model

The cimetidine PBPK model was developed by implementing several modifications to the metformin PBPK model (**Figure 1b**, **Supplemental Text**). At physiological pHs, cimetidine (pKa of 6.9) can exist as both ionized and unionized, and their fractions were calculated using the Henderson–Hasselbalch equation (**Table S3**).[24,33] To calculate γ_h, γ_r, and γ_{urine} of cimetidine using Eq. 10, λ was set to be 0.1 as described previously.[29]

DDI simulation

DDI simulation was performed by combining the developed metformin and cimetidine PBPK models. Cimetidine was assumed to be a competitive inhibitor in the transport of metformin by OCT1, OCT2, or MATEs, as shown in Eq. 15:

$$PS_{act}(+I) = \frac{PS_{act}(\text{control})}{1 + \frac{[I]}{Ki}} \quad (15)$$

where PS_{act}(control) and $PS_{act}(+I)$ are the intrinsic active clearance of metformin in the absence and the presence of an inhibitor, respectively, and I is the inhibitor concentration.

In vitro Ki (or half maximal inhibitory concentration (IC_{50})) values of cimetidine were obtained from the reports where

Table 1 Optimized physiologically-based pharmacokinetic model parameters (k_a, k_{trans}, and $R_{MATE/dif}$) after fitting to the oral metformin doses of 1,500 and 250 mg using differing β_{kidney} values

1,500 mg metformin

		β_{kidney}			
	Observed[6]	**0.1**	**0.3**	**0.5**	**0.8**
$R_{MATE/dif}$	–	153 ± 18.1	213 ± 25.5	325 ± 39.2	814 ± 111
k_a (/hour)	–	0.21 ± 0.013	0.21 ± 0.013	0.21 ± 0.013	0.21 ± 0.013
k_{trans} (/hour)	–	2.4 ± 0.36	2.4 ± 0.36	2.4 ± 0.36	2.4 ± 0.36
AUC_{0-24} (mg•h/L)	21.4 ± 3.18	20.1	20.1	20.2	20.2
CLr (L/hour)	23.0 ± 3.87	29.8	29.8	30	30

250 mg metformin

		β_{kidney}			
	Observed[16]	**0.1**	**0.3**	**0.5**	**0.8**
$R_{MATE/dif}$	–	183 ± 30.1	261 ± 43.3	402 ± 66.3	1,143 ± 186
k_a (/hour)	–	0.21	0.21	0.21	0.21
k_{trans} (/hour)	–	0.61 ± 0.044	0.61 ± 0.044	0.61 ± 0.044	0.61 ± 0.044
AUC_{0-12} (mg•hour/L)	3.75 ± 1.43	4.12	4.12	4.12	4.12
CLr (L/hour)	31.6 ± 9.90	28.5	28.6	28.6	28.6
C_{max} (μg/L)	590 ± 240	502	502	502	502
T_{max} (hour)	3.3 ± 0.8	3.72	3.72	3.72	3.72

AUC_{0-24}, area under the curve from 0–24 hours; AUC_{0-12}, area under the curve from 0–12 hours; CLr, renal clearance; C_{max}, maximum plasma concentration; T_{max}, time of maximum concentration; k_a,absorption rate; k_{trans}, the rate from transit compartment to intestine compartment; $R_{MATE/dif}$, the ratio of the intrinsic clearance of MATEs to the intrinsic passive diffusion clearance via efflux out of cells to the urinary lumen.

the metformin concentration was sufficiently lower than its K_m value (**Table 2**).

The Numeric Analysis Program for Pharmacokinetics (version 2.31)[34] was used for simulation and optimization of parameters using the nonlinear least-squares method. The weight for the calculation was set as 1 (the square root of the value).

RESULTS

Metformin PBPK model

The k_a, k_{trans}, and $R_{MATE/dif}$ were optimized by fitting the model to the time profiles of plasma and blood concentrations and urinary excretion of metformin after a single oral dose of 1,500 mg metformin[6] at varying β_{kidney} values (**Table 1**). Although the optimized $R_{MATE/dif}$ varied from 150–800 at different β_{kidney} values, the optimized k_a and k_{trans} were 0.21 ± 0.01 $hour^{-1}$ and 2.4 ± 0.4 $hour^{-1}$, respectively, regardless of β_{kidney} values. The use of these optimized parameters well reproduced the observed data, including the increase of blood-to-plasma ratios over time (likely from slow distribution of metformin to erythrocytes; **Figure 2a–d**, **Figure S1**). Next, the k_{trans} and $R_{MATE/dif}$ were optimized by fitting the model to the plasma concentration-time profile after oral metformin dosing of 250 mg[16] (intestinal availability adjusted to 0.84 as described in the Methods section) using differing β_{kidney} values (**Figure 2e–h**, **Table 1**). The use of the optimized parameters yielded simulated T_{max} (3.72 hours) and AUC_{0-12} (4.12 mg•h/L) comparable with the observed values (3.3 ± 0.8 hours and 3.75 ± 1.43 mg•h/L, respectively) at all four β_{kidney} values.

Cimetidine PBPK model

Parameters for the cimetidine PBPK model were from the reported data (**Table S4**)[1,10,27,30] and used with no further optimization. Our PBPK model yielded the simulation results that well reproduced the observed data after a single oral administration of 400 mg cimetidine (**Figure 2i**).[18] The simulated AUC (9.10 mg•h/L) was comparable with the observed value (10.4 ± 2 mg•h/L).

DDI simulation

The pharmacokinetic profiles under DDI conditions were simulated using the developed PBPK models for metformin and cimetidine and *in vitro* Ki values (geometric mean) of cimetidine for OCT1, OCT2, and MATEs at differing β_{kidney} values. The simulated plasma concentrations of metformin were increased with coadministration of cimetidine at all β_{kidney} values, but the extent of the changes showed some discrepancies between the simulated and observed values; the fold changes of AUC, C_{max}, and CLr in the simulations were 1.07–1.23, 1.08–1.32, and 0.75–0.90, respectively, whereas the observed fold changes were 1.47, 1.72, and 0.72, respectively (**Table 2**, **Figure S2**).

Sensitivity analysis for *in vitro* Ki values of cimetidine for OCT2 and MATEs

As the reported *in vitro* Ki values of cimetidine for OCT2 and MATEs vary widely (**Table 2**),[10,11,20–22,35–37] we conducted sensitivity analyses for Ki values. DDI simulations were initially conducted with three *in vitro* Ki values for OCT2 (72.6, 509, and 159 μM, corresponding to the smallest and largest

Table 2 Sensitivity analysis for AUC, C_{max}, and CLr ratios between control and drug–drug interaction conditions using different Ki values for OCT2 and MATEs

Sensitivity analysis of three different Ki values for OCT2 (72.6, 509, and 159 represent the lowest and highest values and the geometric mean of *in vitro* Ki values, respectively) and differing β_{kidney} values. The Ki value for MATEs was fixed at the geometric mean value.

		β_{kidney} = 0.1			β_{kidney} = 0.3			β_{kidney} = 0.5			β_{kidney} = 0.8		
		Ki for OCT2 (μM)			Ki for OCT2 (μM)			Ki for OCT2 (μM)			Ki for OCT2 (μM)		
	Observed[16]	72.6	159	509	72.6	159	509	72.6	159	509	72.6	159	509
AUC ratio	1.47 ± 0.75	1.23	1.23	1.23	1.19	1.19	1.19	1.14	1.14	1.14	1.07	1.07	1.07
C_{max} ratio	1.72 ± 0.97	1.32	1.32	1.32	1.26	1.26	1.26	1.19	1.19	1.19	1.08	1.08	1.08
CL_r ratio	0.72 ± 0.32	0.75	0.75	0.75	0.80	0.80	0.80	0.84	0.84	0.84	0.90	0.90	0.90

Sensitivity analysis of three different Ki values for MATEs (1.22, 13.5, and 3.93 represent the lowest and highest values and the geometric mean of *in vitro* Ki values, respectively) and differing β_{kidney} values. The Ki value for OCT2 was fixed at the geometric mean value.

		β_{kidney} = 0.1			β_{kidney} = 0.3			β_{kidney} = 0.5			β_{kidney} = 0.8		
		Ki for MATEs (μM)			Ki for MATEs (μM)			Ki for MATEs (μM)			Ki for MATEs (μM)		
	Observed[16]	1.22	3.93	13.5	1.22	3.93	13.5	1.22	3.93	13.5	1.22	3.93	13.5
AUC ratio	1.47 ± 0.75	1.44	1.23	1.10	1.40	1.19	1.07	1.30	1.14	1.05	1.15	1.07	1.03
C_{max} ratio	1.72 ± 0.97	1.57	1.32	1.13	1.52	1.26	1.09	1.41	1.19	1.07	1.21	1.08	1.03
CL_r ratio	0.72 ± 0.32	0.59	0.75	0.89	0.63	0.80	0.92	0.70	0.84	0.94	0.82	0.90	0.97

The geometric mean and the ranges of the reported *in vitro* Ki (μM) values of cimetidine were as follows: OCT1, 104[11]; OCT2, 159, 72.6–509[10,11,20,21,34,35]; MATEs, 3.93, 1.22–13.5[20–22,41].

AUC, area under the curve; Ki, inhibition constant; C_{max}, maximum plasma concentration; CLr, renal clearance; $\beta_{kidney} = PS_{urine}/(PS_{r,eff}+PS_{urine})$; OCT2, organic cation transporter 2; MATEs, multidrug and toxin extrusion proteins.

values and the geometric mean of the reported values, respectively), whereas the Ki values for OCT1 and MATEs were fixed to the geometric means of 104 μM and 3.93 μM, respectively. The fold changes of AUC, C_{max}, and CLr were not impacted by the Ki values for OCT2 regardless of β_{kidney} values (**Table 2**). DDI simulations were also conducted with three *in vitro* Ki values for MATEs (1.22, 13.5, and 3.93 μM, corresponding to the smallest and largest values and the geometric mean of the reported values, respectively), whereas the Ki values of cimetidine for OCT1 and OCT2 were fixed to 104 μM and 159 μM, respectively. The fold changes in AUC, C_{max}, and CLr were impacted by the Ki values for MATEs (**Table 2**).

Estimation of the *in vivo* Ki value of cimetidine for MATEs

The *in vivo* Ki value of cimetidine for MATEs was estimated by fitting to clinical DDI data with k_{trans} and $R_{MATE/dif}$ fixed to their optimized values at varying β_{kidney} values. Simulation using the estimated *in vivo* Ki values for MATEs at all four β_{kidney} values reproduced the observed fold changes in AUC, CLr, and C_{max} with less than 15% differences (**Figure 3**, **Table 3**). The good agreement between the simulated and observed profiles regardless of β_{kidney} values appears to be consistent with our initial trial on reliable β_{kidney} estimation by fitting to the clinical metformin pharmacokinetic data. The estimated *in vivo* Ki values for MATEs were in the range of the *in vitro* reported Ki values with β_{kidney} values of 0.1 and 0.3 but not with 0.5 and 0.8 (corresponding to 0.52- and 0.18-fold of the smallest *in vitro* reported Ki value (1.22 μM), respectively).

Sensitivity analysis of Ki values of cimetidine for MATEs

For comparison with the previously reported model,[1] we examined the impact of changing Ki values for MATEs on the fold changes in plasma AUC, CLr, or AUC in the proximal tubule cell segment 1 under DDI conditions. Initially, the sensitivity analysis of our PBPK model (β_{kidney} of 0.1) was compared with that of the conventional and electrochemical models reported previously (**Figure 4a–c**).[1] In our model, β_{kidney} values reflect the rate-determining step of renal secretion in proximal tubule cells. Upon additional sensitivity analysis using varying β_{kidney} values (**Figure 4d–f**), the sensitivity to changing Ki values for MATEs on plasma AUC, CLr, and AUC in proximal tubule segment 1 in our model tended to be greater than the previously reported model[1] except for the extreme ends of the β_{kidney} ranges tested. For the plasma AUC of metformin, the observed fold change (1.47) under DDI conditions was recovered by lowering the Ki values for MATEs by ~ 1.5, 2.5, and 6-fold from the smallest *in vitro* Ki value with β_{kidney} values of 0.3, 0.5, and 0.8, respectively (**Figure 4d**). With a β_{kidney} of 0.1, the lowest reported Ki value (1.22 μM) yielded the observed 1.44-fold change in the plasma AUC, close to the observed value. For the CLr, the observed fold change (0.72) was recovered using the Ki values for MATEs that fell within the range of the reported *in vitro* Ki values except for a β_{kidney} of 0.8; for a β_{kidney} of 0.8, the Ki for MATEs had to be lowered to 0.40 μM (approximately threefold lower than the smallest *in vitro* Ki value; **Figure 4e**). For the AUC in proximal tubule segment 1, the fold change under DDI conditions was not available, but as β_{kidney} values increased, so did the sensitivity to changing Ki values

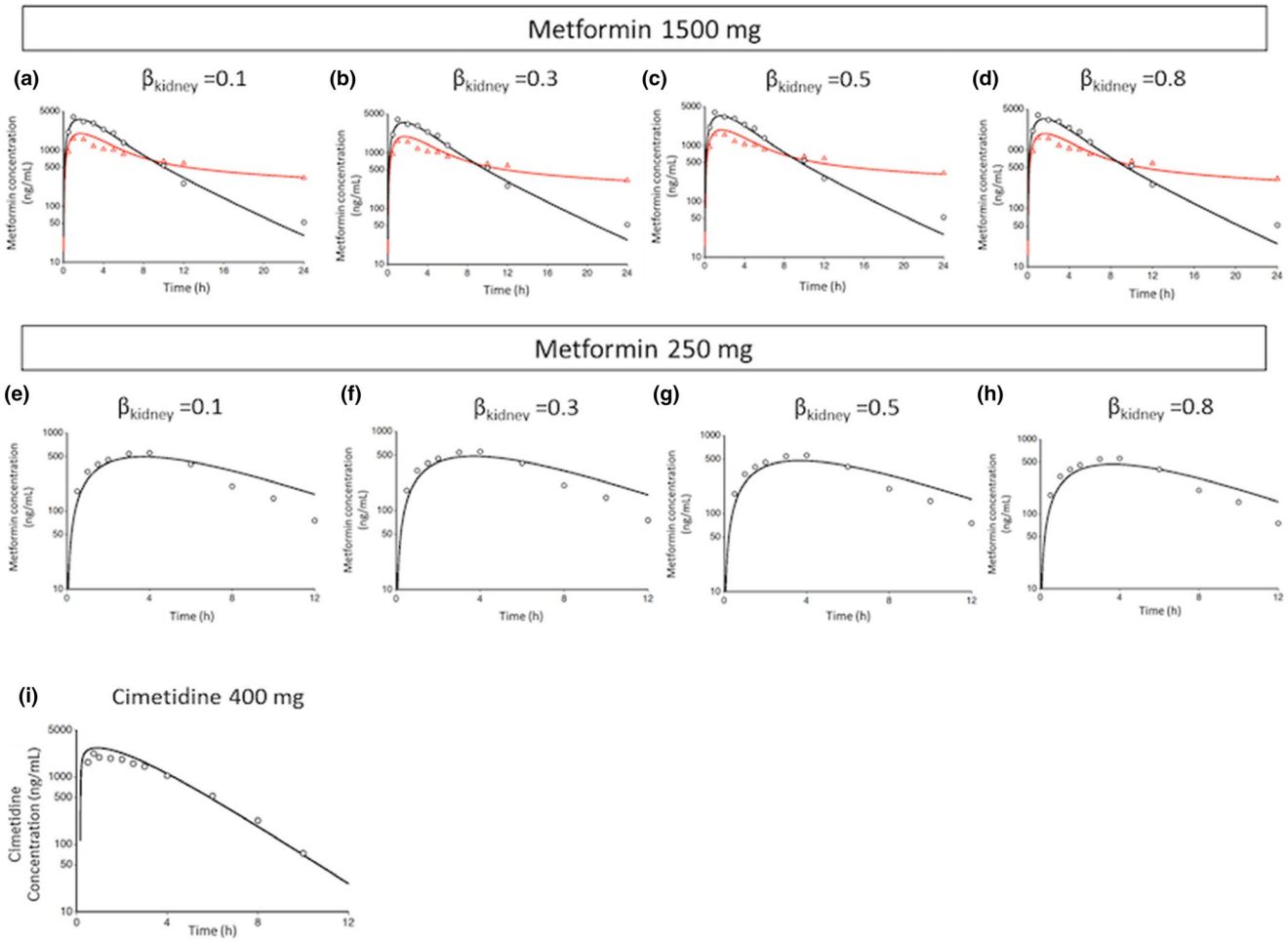

Figure 2 Fitted and observed metformin plasma and blood concentration-time profiles after single oral administration of 1,500 mg metformin (**a–d**), fitted and observed plasma concentration-time profiles after a single oral administration of 250 mg metformin (**e–h**) and after a single oral administration of 400 mg cimetidine (**i**). The black circles and red triangles represent the observed concentration-time profiles in plasma and blood, respectively. The black and red lines represent the fitted concentration-time profiles in plasma and blood, respectively. Simulations were performed using differing β_{kidney} values; $\beta_{kidney} = PS_{urine}/(PS_{r,eff}+PS_{urine})$.

for MATEs increase (**Figure 4f**). Overall, the observed fold changes in the plasma AUC or CLr were reproduced using the Ki values for MATEs near and within the range of those obtained *in vitro* with β_{kidney} values of 0.1, 0.3, or 0.5 but not 0.8.

DISCUSSION

Metformin is a clinically important antidiabetic drug and often used as a probe drug to examine the potential DDI mediated by renal transporters. Thus, there is a clear need to establish and refine PBPK models that can accurately and quantitatively predict the DDI potential between metformin and other drugs using *in vitro* data. To this end, the previous metformin PBPK model ("electrochemical model")[1] incorporated the transport process by OCTs driven by dynamically changing membrane potential in response to metformin levels. This electrochemical model reproduced the plasma concentration profile of metformin alone, but the extent of the fold changes in the plasma AUC under DDI conditions was recovered only when the Ki value for MATEs was set at 8.7-fold lower values than the geometric mean value of the reported *in vitro* Ki values (3.93 μM). Although *in vitro* Ki values can substantially vary, the 8.7-fold difference is rather substantial. To reconcile these differences, our model considered the electrogenic property of OCTs but kept the membrane potential constant. In the living cells and organisms, the electrochemical potential is regulated by concentration and permeability of multiple ions (e.g., potassium ion, sodium ion, chloride ion, typically at 100–200 mM) present at much higher concentrations.[38] Thus, a reasonable assumption may be that drug-induced changes in the electrochemical potential at the therapeutically relevant level to be modest extent. Our current PBPK model yielded *in vivo* simulated Ki values within the reported *in vitro* Ki values when β_{kidney} was 0.1 or 0.3 (**Table 3**). In the sensitivity analysis, the observed plasma AUC change was reproduced within 15% difference (**Table 2**) with the lowest *in vitro* Ki values and observed CLr change was reproduced in the range of *in vitro* Ki values (1.22–5 μM) except for a β_{kidney} of 0.8 (**Figure 4e**). Overall, our model reproduced

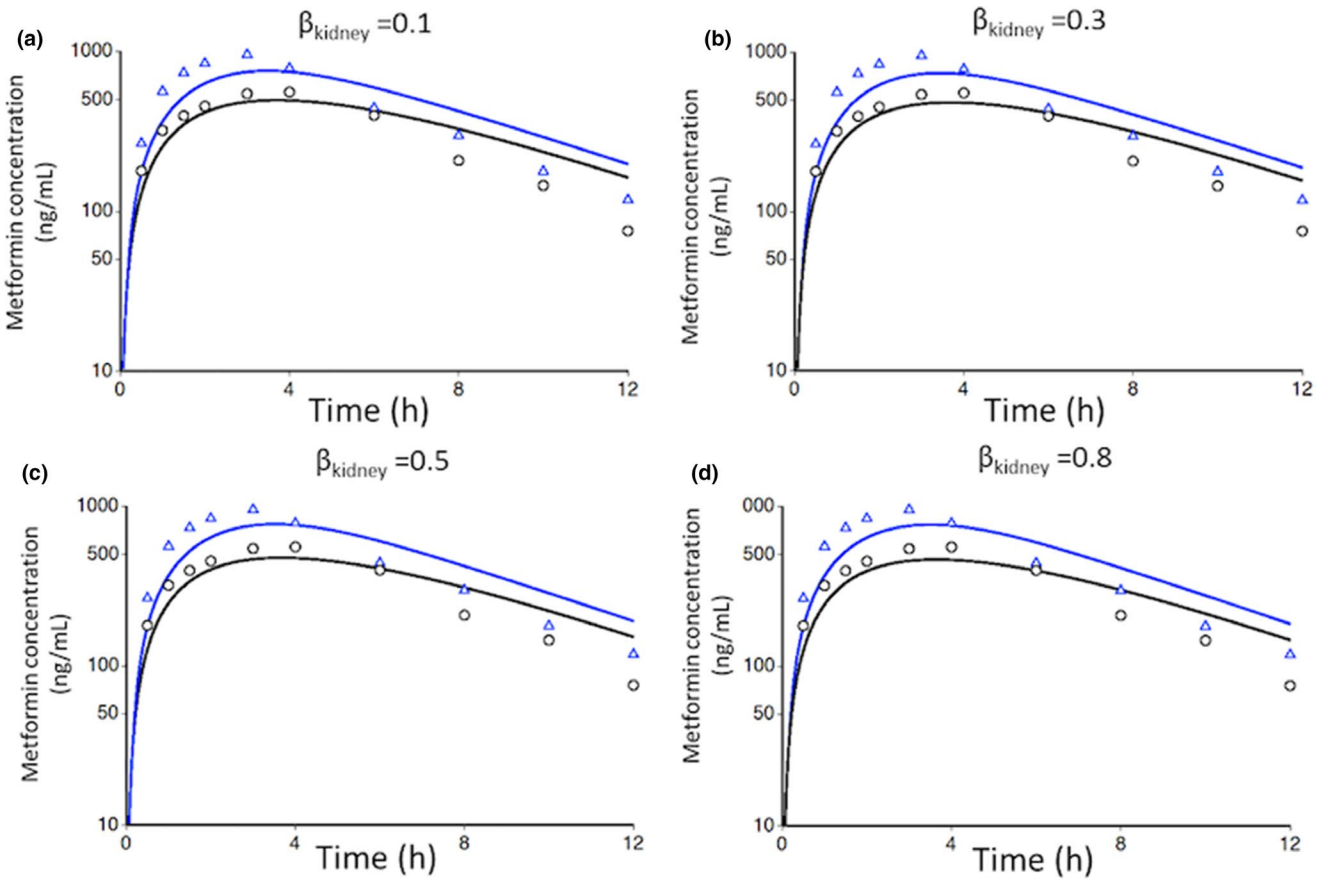

Figure 3 Metformin plasma concentration-time profiles under control and drug–drug interaction conditions using fitted *in vivo* inhibition constant values for multidrug and toxin extrusion proteins after oral administration of 250 mg metformin and 400 mg cimetidine. For the control condition, the optimized parameters shown in **Table 1** for β_{kidney} value of 0.1 (**a**), 0.3 (**b**), 0.5 (**c**), or 0.8 (**d**) were used. For drug–drug interaction conditions, the optimized parameters were fixed, but the β_{kidney} value was not fixed and allowed to change as the renal transport processes became inhibited. The black circles and blue triangles represent the observed plasma concentrations under control and drug–drug interaction conditions, respectively, and the black and blue lines represent the corresponding simulation results; $\beta_{kidney} = PS_{urine}/(PS_{r,eff}+PS_{urine})$.

Table 3 Observed and simulated AUC, C_{max}, and CL_r ratios of metformin between control and drug–drug interaction conditions with fitted *in vivo* Ki value for MATEs at various β_{kidney} values

β_{kidney}[a]	Fitted *in vivo* Ki value for MATEs (μM)	Fold changes from simulations		
		AUC (1.47 ± 0.75)[16]	C_{max} (1.72 ± 0.97)[16]	CL_r (0.72 ± 0.32)[16]
0.1	1.71 ± 0.74	1.40	1.52	0.63
0.3	1.34 ± 0.60	1.39	1.50	0.64
0.5	0.64 ± 0.34	1.42	1.54	0.61
0.8	0.23 ± 0.12	1.42	1.54	0.61

AUC, area under the curve; C_{max}, the maximum plasma concentration; CLr, renal clearance; Ki, inhibition constant; MATEs, multidrug and toxin extrusion proteins.
[a]For the control condition, the β_{kidney} value was set to 0.1, 0.3, 0.5, or 0.8, and the optimized parameters shown in **Table 1** were used. For the drug–drug interaction conditions, the optimized parameters were fixed, but the β_{kidney} value was not fixed and allowed to change as the renal transport processes became inhibited.

the clinical DDI data of metformin and cimetidine with *in vitro* Ki values when β_{kidney} was 0.3 or less. In addition, the results from sensitivity analysis were comparable between the previous electrochemical model and our model with a β_{kidney} of 0.8 (**Figure 4b,d,e**). These results suggest that the rate-determining step in the electrochemical model is likely the renal uptake, requiring one to greatly lower the Ki value for MATEs or OCT2 from *in vitro* Ki values to reproduce the observed DDI data. Thus, a β_{kidney} of 0.3 or less is recommended for future efforts to predict the potential DDI using *in vitro* Ki values. Of note, we could not obtain reliable β_{kidney} estimates by fitting to clinical metformin data

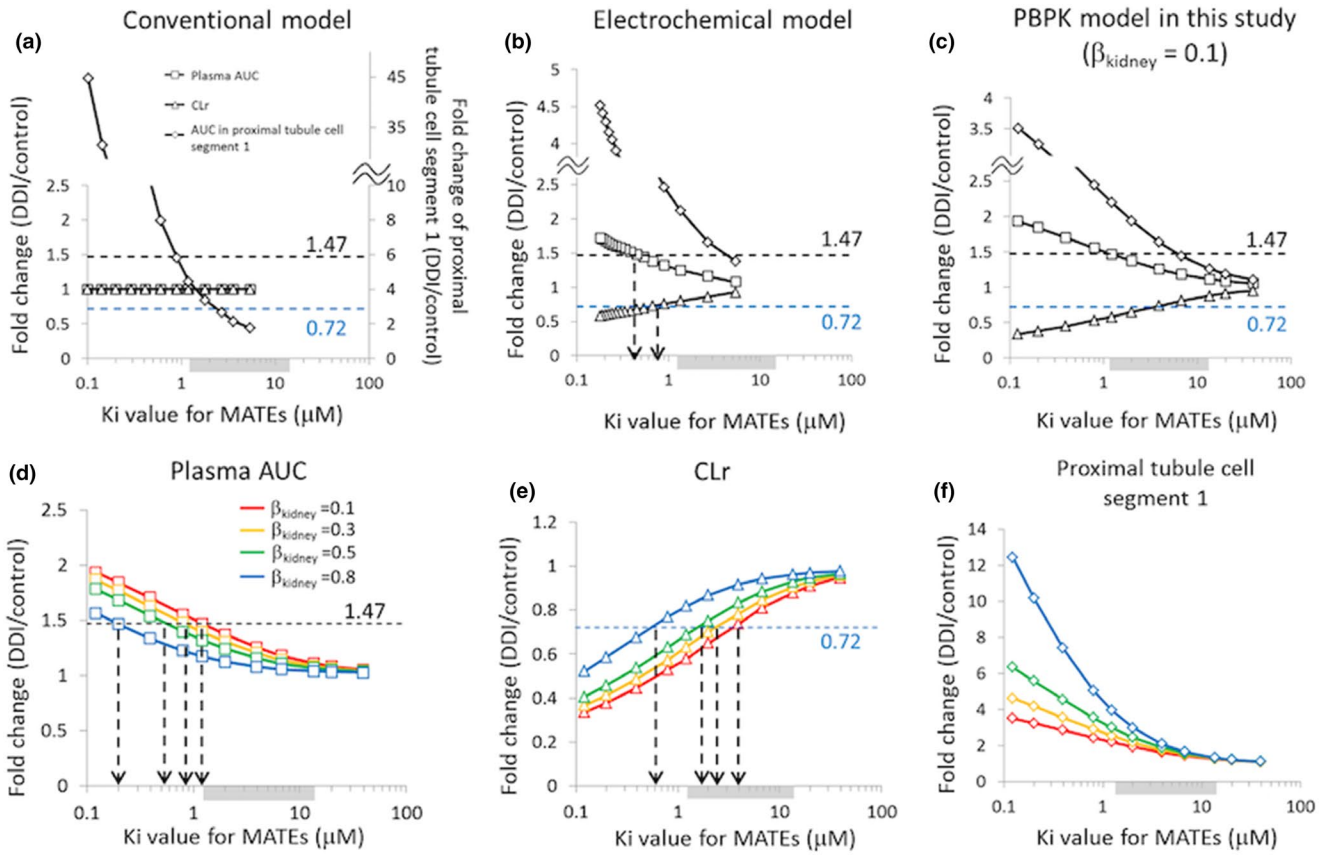

Figure 4 Sensitivity analysis to examine the impact of changing Ki values for MATEs on the fold changes in plasma AUC (□), CLr (△), or AUC in the proximal tubule cell segment 1 (◇). For comparison, the initial analysis was performed using the conventional model (**a**) and the electrochemical model (**b**) reported by Burt *et al.*[1] and our current PBPK model (**c**) using β_{kidney} = 0.1. For our current PBPK model, the impact of changing β_{kidney} values was examined on plasma AUC (**d**), CLr (**e**), and AUC in the proximal tubule cell segment 1 (**f**). The shaded area near the *x*-axis indicates the range of *in vitro* Ki values for MATEs reported in the literature (geometric mean: 3.93 μM (1.22–13.5 μM)). The dotted horizontal lines indicate the observed fold changes in plasma AUC (1.47, black) or CLr (0.72, blue). (**d–f**) Red, orange, green, and blue symbols and lines represent the simulation results using optimized values shown in **Table 1** for β_{kidney} values of 0.1, 0.3, 0.5, and 0.8, respectively. DDI, drug–drug interaction; Ki, inhibition constant; MATEs, multidrug and toxin extrusion proteins; PBPK, physiologically-based pharmacokinetic. AUC, area under the curve; CLr, renal clearance; $\beta_{kidney} = PS_{urine}/(PS_{r,eff}+PS_{urine})$.

(under control conditions). Our approach was to use a wide range of fixed β_{kidney} values (to cover situations with differing rate-determining steps) under control conditions and to deduce optimal β_{kidney} ranges from sensitivity analysis. This approach may represent another strategy to indirectly estimate β_{kidney}.

In understanding how our model was capable of reproducing the clinical DDI data using *in vitro* Ki values and small β_{kidney} values, a mechanistic interpretation of the β_{kidney} values may shed some light on possible reasons. The extended clearance concept takes all intrinsic processes into account when assessing the overall elimination process. Incorporating the extended clearance concept, $CL_{int,sec}$ is described as $PS_{r,inf}.\beta_{kidney}$ (Eq. 7). By converting the parameters with Eqs. 5 and 8–14, $CL_{int,sec}$ can be transformed to Eq. 16.

$$CL_{int,sec} = \left(PS_{OCT2,inf} + PS_{r,dif,inf}\right) * \frac{PS_{MATE}+PS_{urine,dif,eff}}{\frac{e^N}{R_{OCT2,inf/eff}}PS_{OCT2,inf}+PS_{r,dif,eff}+PS_{MATE}+PS_{urine,dif,eff}} \quad (16)$$

When β_{kidney} is 0.1, the values for individual parameters in Eq. 16 are as follows: $PS_{OCT2,inf}$, 732 L/hour; $PS_{r,dif,inf}$, 0.043 L/hour; $PS_{r,dif,eff}$, 0.0031 L/hour; PS_{MATE}, 4.47 L/hour; $PS_{urine,dif,eff}$, 0.024 L/hour; $e^N/R_{OCT2,inf/eff}$, 0.055. When the transport of metformin by MATEs becomes inhibited to 20% in the presence of cimetidine (i.e., PS_{MATE} decreased to 0.89 L/hour), the β_{kidney} is changed from 0.1 to 0.022, and $CL_{int,sec}$ is decreased from 73.5 to 16.3 L/hour, by ~ 4.5-fold when compared with the control condition. A similar calculation can be performed when β_{kidney} is 0.8. The values for individual parameters in Eq. 16 are as follows: $PS_{OCT2,inf}$, 126 L/hour; $PS_{r,dif,inf}$, 0.043 L/hour; $PS_{r,dif,eff}$, 0.0031 L/hour; PS_{MATE}, 27.9 L/hour; $PS_{urine,dif,eff}$, 0.024 L/hour; $e^N/R_{OCT2,inf/eff}$, 0.055. When the transport of metformin by MATEs becomes inhibited to 20% in the presence of cimetidine (i.e., PS_{MATE} decreased to 5.6 L/hour), β_{kidney} is changed from 0.8 to 0.45, and $CL_{int,sec}$ is decreased from 101 to 56.4 L/hour, by ~ 1.8-fold when compared with the control condition. These calculation results indicate that as β_{kidney} values become smaller, the inhibition of MATEs has a much greater impact on $CL_{int,sec}$.

A number of DDI cases have been reported between metformin and other drugs that can inhibit both OCT2 and MATEs (e.g., pyrimethamine,[39,40] dolutegravir,[41] trimethoprim,[37,42] and vandetanib[43]). For pyrimethamine, *in vitro* Ki values for MATEs (0.059–0.15 μM) are much lower than those for OCT2 (4.1–23 μM).[22,38,44] The observed C_{max} values of unbound pyrimethamine in plasma range from 0.30–0.40 μM after a 50 mg oral pyrimethamine dose,[35,45] suggesting the inhibition of MATEs as the likely DDI mechanism. In the case of dolutegravir, its *in vitro* Ki values for OCT2 and MATE1 are 1.9 and 6.3 μM,[41] respectively. In a clinical DDI study, the coadministration of dolutegravir increased the plasma AUC of metformin by 79% and 145% when dolutegravir was coadministered as a single daily dose of 50 mg and two daily doses of 50 mg with a 12-hour interval.[41] With its unbound C_{max} values being much lower than the *in vitro* Ki values for OCT2 and MATE1, the inhibitions of OCT2 and MATE1 were deemed unlikely to explain the observed DDI, and the exact mechanism remains unknown. Our current PBPK model may aid the efforts to quantitatively predict the DDI and gain mechanistic insights into complex DDI cases between metformin and other drugs.

Our PBPK model for metformin may also have some utility in understanding the source of variable response and toxicity to metformin therapy. Drug concentrations in plasma or blood are often assumed to be associated with drug efficacy and toxicity. It is, however, increasingly recognized that it may not be the case if a drug is actively taken up into tissues or metabolized in the tissues.[46] Although one third of patients did not respond to metformin,[2,3] the metformin levels in plasma are not predictive of blood lactate concentrations and the risk for lactic acidosis.[4,15,47] In addition, the diabetic patients carrying the MATE1 promoter variant (g.-66T→C) exhibit a greater response to metformin than those carrying the wildtype.[15] By incorporating variables consistent with biologically plausible mechanisms (especially variables for transport processes by OCT1/2 and MATEs), it might be possible to gain mechanistic insights into interindividual variations in metformin response and side effects and to predict the pharmacokinetic profiles and clinical outcomes using the virtual clinical study method.[48]

In conclusion, we developed a refined PBPK model for metformin that successfully reproduced the DDI between metformin and cimetidine with *in vitro* Ki values. Our results supported the fact that the DDI between metformin and cimetidine is likely mediated by the inhibition of MATEs by cimetidine rather than by OCT2 inhibition.

Supporting Information. Supplementary information accompanies this paper on the *CPT: Pharmacometrics & Systems Pharmacology* website (www.psp-journal.com).

Figure S1. Simulated (lines) and observed (open circles) time profiles of metformin urinary excretion after a single oral administration of 1,500 mg metformin using various β_{kidney} values.
Figure S2. Metformin plasma concentration time profiles of control and drug–drug interaction conditions using the lowest and geometric mean of inhibition constant values of cimetidine at differing β_{kidney} values after the administration of 250 mg metformin and 400 mg cimetidine.
Table S1. Various parameters used in the metformin physiologically-based pharmacokinetic model and reported *in vitro* Km values for transporters of metformin parameters used in the metformin physiologically-based pharmacokinetic model.
Table S2. Physiological parameters of blood volume, tissue volumes, hematocrit value, and blood flows.
Table S3. Physiological parameters, membrane potential, blood flow, and urinary flow in the kidney model.
Table S4. Parameters used in the cimetidine physiologically-based pharmacokinetic model.
Supplementary Material S1. Model code file.
Supplementary Material S2. Model equations for metformin.

Funding. No funding was received for this work.

Conflict of Interest. The authors declared no competing interests for this work.

Author Contributions. K.N., K.T., W.L., N.I., B.B., and Y.S. wrote the manuscript. K.N., K.T., and Y.S. designed the research. K.N., K.T., and Y.S. performed the research. K.N., K.T., and Y.S. analyzed the data.

1. Burt, H.J. *et al.* Metformin and cimetidine: physiologically based pharmacokinetic modelling to investigate transporter mediated drug-drug interactions. *Eur. J. Pharm. Sci.* **88**, 70–82 (2016).
2. Graham, G.G. *et al.* Clinical pharmacokinetics of metformin. *Clin. Pharmacokinet.* **50**, 81–98 (2011).
3. Shikata, E. *et al.* Human organic cation transporter (*OCT1* and *OCT2*) gene polymorphisms and therapeutic effects of metformin. *J. Hum. Genet.* **52**, 117–122 (2007).
4. Lalau, J.D. & Race, J.M. Lactic acidosis in metformin-treated patients. Prognostic value of arterial lactate levels and plasma metformin concentrations. *Drug Saf.* **20**, 377–384 (1999).
5. Pentikainen, P.J., Neuvonen, P.J. & Penttila, A. Pharmacokinetics of metformin after intravenous and oral administration to man. *Eur. J. Clin. Pharmacol.* **16**, 195–202 (1979).
6. Tucker, G.T., Casey, C., Phillips, P.J., Connor, H., Ward, J.D. & Woods, H.F. Metformin kinetics in healthy subjects and in patients with diabetes mellitus. *Br. J. Clin. Pharmacol.* **12**, 235–246 (1981).
7. Rena, G., Pearson, E.R. & Sakamoto, K. Molecular mechanism of action of metformin: old or new insights? *Diabetologia* **56**, 1898–1906 (2013).
8. Stage, T.B., Brøsen, K. & Christensen, M.M. A comprehensive review of drug–drug interactions with metformin. *Clin. Pharmacokinet.* **54**, 811–824 (2015).
9. Xie, F., Ke, A.B., Bowers, G.D. & Zamek-Gliszczynski, M.J. Metformin's intrinsic blood-to-plasma partition ratio (B/P): reconciling the perceived high *in vivo* B/P > 10 with the *in vitro* equilibrium value of unity. *J. Pharmacol. Exp. Ther.* **354**, 225–229 (2015).
10. Umehara, K.I., Iwatsubo, T., Noguchi, K. & Kamimura, H. Functional involvement of organic cation transporter1 (OCT1/Oct1) in the hepatic uptake of organic cations in humans and rats. *Xenobiotica* **37**, 818–831 (2007).
11. Kimura, N., Okuda, M. & Inui, K. Metformin transport by renal basolateral organic cation transporter hOCT2. *Pharm. Res.* **22**, 255–259 (2005).
12. Tanihara, Y., Masuda, S., Sato, T., Katsura, T., Ogawa, O. & Inui, K. Substrate specificity of MATE1 and MATE2-K, human multidrug and toxin extrusions/H(+)-organic cation antiporters. *Biochem. Pharmacol.* **74**, 359–371 (2007).
13. Christensen, M.M. *et al.* The pharmacogenetics of metformin and its impact on plasma metformin steady-state levels and glycosylated hemoglobin A1c. *Pharmacogenet. Genomics* **21**, 837–850 (2011).
14. Christensen, M.M. *et al.* A gene-gene interaction between polymorphisms in the OCT2 and MATE1 genes influences the renal clearance of metformin. *Pharmacogenet. Genomics* **23**, 526–534 (2013).
15. Stocker, S.L. *et al.* The effect of novel promoter variants in MATE1 and MATE2 on the pharmacokinetics and pharmacodynamics of metformin. *Clin. Pharmacol. Ther.* **93**, 186–194 (2013).
16. Somogyi, A., Stockley, C., Keal, J., Rolan, P. & Bochner, F. Reduction of metformin renal tubular secretion by cimetidine in man. *Br. J. Clin. Pharmacol.* **23**, 545–551 (1987).

17. Wang, Z.J., Yin, O.Q., Tomlinson, B. & Chow, M.S. OCT2 polymorphisms and *in-vivo* renal functional consequence: studies with metformin and cimetidine. *Pharmacogenet. Genomics* **18**, 637–645 (2008).
18. Grahnén, A., von Bahr, C., Lindström, B. & Rosén, A. Bioavailability and pharmacokinetics of cimetidine. *Eur. J. Clin. Pharmacol.* **16**, 335–340 (1979).
19. Somogyi, A., Thielscher, S. & Gugler, R. Influence of phenobarbital treatment on cimetidine kinetics. *Eur. J. Clin. Pharmacol.* **19**, 343–347 (1981).
20. Elsby, R. *et al.* Mechanistic *in vitro* studies confirm that inhibition of the renal apical efflux transporter multidrug and toxin extrusion (MATE) 1, and not altered absorption, underlies the increased metformin exposure observed in clinical interactions with cimetidine, trimethoprim or pyrimethamine. *Pharmacol. Res. Perspect.* **5** (2017). https://doi.org/10.1002/prp2.357
21. Ito, S. *et al.* Competitive inhibition of the luminal efflux by multidrug and toxin extrusions, but not basolateral uptake by organic cation transporter 2, is the likely mechanism underlying the pharmacokinetic drug-drug interactions caused by cimetidine in the kidney. *J. Pharmacol. Exp. Ther.* **340**, 393–403 (2012).
22. Shen, H. *et al.* Characterization of organic anion transporter 2 (SLC22A7): a highly efficient transporter for creatinine and species-dependent renal tubular expression. *Drug Metab. Dispos.* **43**, 984–993 (2015).
23. Watanabe, T., Kusuhara, H., Maeda, K., Shitara, Y. & Sugiyama, Y. Physiologically based pharmacokinetic modeling to predict transporter-mediated clearance and distribution of pravastatin in humans. *J. Pharmacol. Exp. Ther.* **328**, 652–662 (2009).
24. Yoshikado, T. *et al.* Quantitative analyses of hepatic OATP-mediated interactions between statins and inhibitors using PBPK modeling with a parameter optimization method. *Clin. Pharmacol. Ther.* **100**, 513–523 (2016).
25. Futatsugi, A., Toshimoto, K., Yoshikado, T., Sugiyama, Y. & Kato, Y. Evaluation of alteration in hepatic and intestinal BCRP function *in vivo* from ABCG2 c.421C>a polymorphism based on PBPK analysis of Rosuvastatin. *Drug Metab. Dispos.* **46**, 749–757 (2018).
26. Rodgers, T., Leahy, D. & Rowland, M. Physiologically based pharmacokinetic modeling 1: predicting the tissue distribution of moderate-to-strong bases. *J. Pharm. Sci.* **94**, 1259–1276 (2005).
27. Chien, H.C. *et al.* Rapid method to determine intracellular drug concentrations in cellular uptake assays: application to metformin in organic cation transporter 1-transfected human embryonic kidney 293 cells. *Drug Metab. Dispos.* **44**, 356–364 (2016).
28. Yoshida, K., Maeda, K. & Sugiyama, Y. Hepatic and intestinal drug transporters: prediction of pharmacokinetic effects caused by drug-drug interactions and genetic polymorphisms. *Annu. Rev. Pharmacol. Toxicol.* **53**, 581–612 (2013).
29. Yoshikado, T. *et al.* Comparison of methods for estimating unbound intracellular-to-medium concentration ratios in rat and human hepatocytes using statins. *Drug Metab. Dispos.* **45**, 779–789 (2017).
30. Balimane, P.V. & Chong, S. Evaluation of permeability and P-glycoprotein interactions: industry outlook. In *Biopharmaceutics Applications in Drug Development* (eds. Krishna, R. and Yu, L.) 101–138 (Springer, New York, 2008).
31. Min, K.A., Zhang, X., Yu, J.Y. & Rosania, G.R. Computational approaches to analyse and predict small molecule transport and distribution at cellular and subcellular levels. *Biopharm. Drug Dispos.* **35**, 15–32 (2014).
32. Scheen, A.J. Clinical pharmacokinetics of metformin. *Clin. Pharmacokinet.* **30**, 359–371 (1996).
33. Siener, R., Jahnen, A. & Hesse, A. Influence of a mineral water rich in calcium, magnesium and bicarbonate on urine composition and the risk of calcium oxalate crystallization. *Eur. J. Clin. Nutr.* **58**, 270–276 (2004).
34. Hisaka, A. & Sugiyama, Y. Analysis of nonlinear and nonsteady state hepatic extraction with the dispersion model using the finite difference method. *J. Pharmacokinet. Biopharm.* **26**, 495–519 (1998).
35. Masuda, S. *et al.* Identification and functional characterization of a new human kidney-specific H+/organic cation antiporter, kidney-specific multidrug and toxin extrusion 2. *J. Am. Soc. Nephrol.* **17**, 2127–2135 (2006).
36. Tsuda, M., Terada, T., Mizuno, T., Katsura, T., Shimakura, J. & Inui, K. Targeted disruption of the multidrug and toxin extrusion 1 (mate1) gene in mice reduces renal secretion of metformin. *Mol. Pharmacol.* **75**, 1280–1286 (2009).
37. Müller, F. *et al.* N(1)-methylnicotinamide as an endogenous probe for drug interactions by renal cation transporters: studies on the metformin-trimethoprim interaction. *Eur. J. Clin. Pharmacol.* **71**, 85–94 (2015).
38. Hodgkin, A.L. & Katz, B. The effect of sodium ions on the electrical activity of giant axon of the squid. *J. Physiol.* **108**, 37–77 (1949).
39. Kusuhara, H. *et al.* Effects of a MATE protein inhibitor, pyrimethamine, on the renal elimination of metformin at oral microdose and at therapeutic dose in healthy subjects. *Clin. Pharmacol. Ther.* **89**, 837–844 (2011).
40. Oh, J. *et al.* Inhibition of the multidrug and toxin extrusion (MATE) transporter by pyrimethamine increases the plasma concentration of metformin but does not increase antihyperglycaemic activity in humans. *Diabetes Obes. Metab.* **18**, 104–108 (2016).
41. Song, *et al.* The effect of dolutegravir on the pharmacokinetics of metformin in healthy subjects. *J. Acquir. Immune Defic. Syndr.* **72**, 400–407 (2016).
42. Grün, B. *et al.* Trimethoprim-metformin interaction and its genetic modulation by OCT2 and MATE1 transporters. *Br. J. Clin. Pharmacol.* **76**, 787–796 (2013).
43. Johansson, S. *et al.* Pharmacokinetic evaluations of the co-administrations of vandetanib and metformin, digoxin, midazolam, omeprazole or ranitidine. *Clin. Pharmacokinet.* **53**, 837–847 (2014).
44. Yin, J., Duan, H. & Wang, J. Impact of substrate-dependent inhibition on renal organic cation transporters hOCT2 and hMATE1/2-K-mediated drug transport and intracellular accumulation. *J. Pharmacol. Exp. Ther.* **359**, 401–410 (2016).
45. Mansor, S.M. *et al.* Single dose kinetic study of the triple combination mefloquine/sulphadoxine/pyrimethamine (Fansimef) in healthy male volunteers. *Br. J. Clin. Pharmacol.* **27**, 381–386 (1989).
46. Chu, X. *et al.* Intracellular drug concentrations and transporters: measurement, modeling, and implications for the liver. *Clin. Pharmacol. Ther.* **94**, 126–141 (2013).
47. Hermann, L.S., Scherstén, B., Bitzén, P.O., Kjellström, T., Lindgärde, F. & Melander, A. Therapeutic comparison of metformin and sulfonylurea, alone and in various combinations. A double-blind controlled study. *Diabetes Care* **17**, 1100–1109 (1994).
48. Toshimoto, K., Tomaru, A., Hosokawa, M. & Sugiyama, Y. Virtual clinical studies to examine the probability distribution of the AUC at target tissues using physiologically-based pharmacokinetic modeling: application to analyses of the effect of genetic polymorphism of enzymes and transporters on irinotecan induced side effects. *Pharm. Res.* **34**, 1584–1600 (2017).